Model-Generated Surface Wind Fields for Storm Surge and Ocean Wave Calculations: A Case Study

Hsiao-ming Hsu[1], Yueh-jiuan G. Hsu[2] and Beng-chun Lee[2]

[1]National Center for Atmospheric Research
P.O. Box 3000
Boulder, Colorado, USA

[2]Central Weather Bureau
64 Kung Yuan Rd.,
Taipei, Taiwan, ROC

1. Introduction

Storm surge and ocean wave models have been able to provide predictions of water level, wave height, wave frequency and wave intensity based on their own nonlinear processes and subgrid-scale parameterizations. One of the important inputs is the surface wind field, which can significantly affect, and sometimes dominate these model results. Accurate predictions from any storm surge and ocean wave model depend heavily on the accuracy of the surface wind field. Therefore, objective prediction of the surface wind field by an atmospheric numerical model becomes a critical path for a successful operation of any storm surge and ocean wave model.

To examine the quality of the model-generated surface wind field, we intend to apply the storm surge and ocean wave models currently operated at CWB/MMC (Central Weather Bureau/Marine Meteorology Center) to the event of Typhoon Herb of 1996, and to compare model results with available observations. The surface wind fields are obtained by simulating Typhoon Herb with the Penn State/NCAR Mesoscale Model Version 5 (MM5). Of course, an accurate surface wind pattern resulted from a typhoon simulation/forecast is a consequence of a successful computation by an atmospheric numerical model. Such success is based on a collective combination of the model dynamics, physics, numerics, and the model initialization. The correct prediction of the hurricane intensity is even a harder task to face for any tropical cyclone modelers and forecasters. It is a great challenge.

As an initial effort, we attempt to investigate the influences of different surface wind patterns to the simulations of storm surge and ocean surface wave. These wind fields are obtained from MM5 simulations of Typhoon Herb with different tropical cyclone initializations

2. Experimental design

The doubly nested computational grids are depicted in Fig. 1. The inner and outer computational grids have mesh sizes of 121x136 and 87x87 points and grid increments of 9 and 27 km, respectively. The nested grids, each with 35 vertical layers, interact during the simulation. Also in Figure 1, the best estimated locations of the eye of Herb are plotted for every six hours.

For both domains, the Betts-Miller technique (Betts and Miller 1993) was chosen for the cumulus parameterization, and the simple ice scheme of Dudhia (1989) for the explicit precipitation calculation. Our choice of the planetary boundary-layer parameterization was the "MRF" technique, which is employed in the Medium-Range Forecast Model of NCEP, and is based on Troen and Mahrt (1986) and Hong and Pan (1996). The model initial conditions were generated by interpolating the 2.5 degree ECMWF global analysis data set. It is apparent that this resolution is too coarse even for the model resolution of the outer domain. A vortex enhancement scheme was applied to the original vortex interpolated from the ECMWF analysis. Then the simulations were carried out for 4 days between 00Z 29/7/1996 and 00Z 2/8/1996, and the outer-domain calculations constantly included the analyzed ECMWF data. In other words, the analyzed fields continuously nudged the calculations of outer domain. The primary purpose of this procedure is to produce some dynamically consistent model data sets. The surface wind fields in these data sets then can be used to test their usefulness in storm surge and ocean wave models.

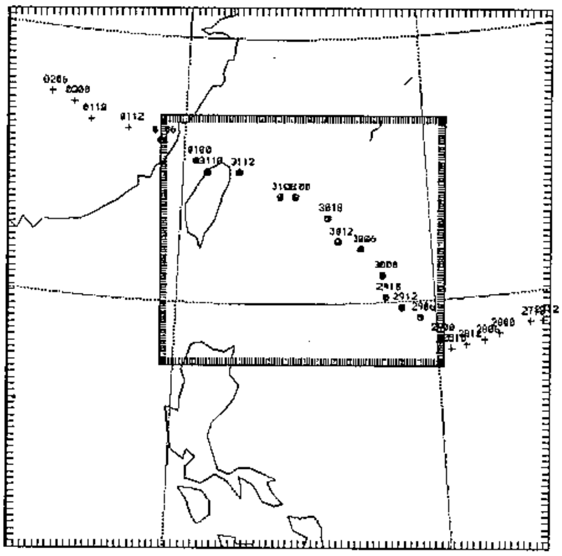

Figure 1. Area coverage for outer and inner domains.

3. Results of the experiments

Two numerical experiments were conducted for this study: one with the original, un-enhanced vortex (ORIV) and the other with the enhanced vortex (MODV). In Figure 2, the tracks of the minimum surface pressure of the simulated typhoons are shown. The ORIV experiment gives the track with thin line and cross symbols, while the track with thick line and plus symbols is resulted from experiment MODV. Both of them indicate very close paths with the observations of every 6 hours shown by circles. Furthermore, both simulated tracks exhibit circular motions as model typhoons move from southeast to northwest. Those loops are primarily caused by the gyration of the polygonal eyes. They are very clearly shown in the animations of the surface pressure patterns. The gyration of the eye of Typhoon Herb has been identified in the radar observations at Wu Fen San station of CWB.

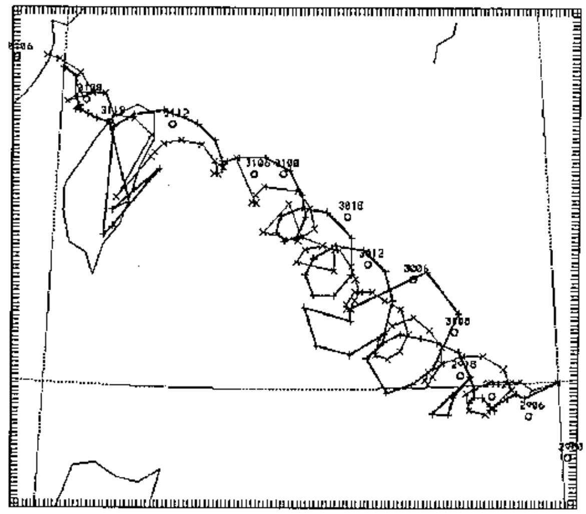

Figure 2. The tracks of the minimum surface pressure. The thick line and the plus symbols are for experiment MODV, and the line and cross symbols for experiment ORIV. The circle symbols are for the observations.

The influence of the Central Mountain Range in Taiwan was significant during the entire event of this typhoon. Before the typhoon reached the island, its center moved in a northwest direction over the western Pacific, and its upstream flow coming from north or northwest toward the island produced a wake region over the southeastern Taiwan in the lee of the mountain (upper panel, Figure 3). After the typhoon moved across the Taiwan Strait over the mainland China, its south or southeast circulation caused another wake region over the northern Taiwan (lower panel, Figure 3). These wakes contained even flow reversals in the lower atmosphere near the surface, and such wakes are well known (Smith and Smith, 1995; Wang, 1980).

During the period Herb was in the vicinity of Taiwan, its circulation was quite interesting at least indicated by the model results. First, as seen from the tracks (Figure 2), both simulations indicate the surface pressure minima were over the eastern side of the island before they moved to the western side. Figure 4 displays the surface pressure patterns over the Taiwan Island and its immediate vicinity from the experiment MODV between 12Z and 18Z, 31/7/1996 when the center of Herb was over the northern island. The region shown in this Figure is only a small portion of the inner computational domain, and 4 panels are 2 hours apart. At 12Z the typhoon center was still over the Pacific. Two hours later, it reached the northeastern corner of the island, and its center pressure increased from 939 mb to 942 mb due to the presence of the mountainous island. The center moved around the northern island to the northwestern side with still increasing center pressure to 948 mb. While this center remained over the northwestern part of the island at 18Z, a secondary center appeared over the eastern coast. This sequence produced by this particular numerical simulation closely follows our current understanding of the event (Shieh *et al.*, 1997). Because of the island and its steep topography, the movement of Herb and its circulation were significantly altered. The surface wind patterns cannot be characterized as an axisymmetric circular pattern. Figure 5 shows the near-surface wind fields for those four instances appearing in Figure 4. Such complexity in surface wind patterns can only be provided by a numerical model with a sufficiently high resolution.

While Herb was in the middle of the transit over the island at 15Z, its surface pressure and wind fields were quite circular as shown in Figure 6. But such circular patterns are definitely not a persistent feature of Herb and most of other tropical cyclones. Therefore, numerical models become even more important in providing detail information on the structures of tropical cyclones than before.

In comparing with observational estimates of the strength of Herb described in Shieh *et al* (1997), the lowest surface pressure and the highest surface wind are extracted from the numerical experiments ORIV and MODV. The upper panel of Figure 7 depicts the time history of the minimum surface pressure. The dots are the observational estimates, and solid and dashed lines are resulted from ORIV and MODV, respectively. Although the enhanced vortex produced much lower surface pressure, the observed was still lower. On the other hand, the simulation with the un-enhanced vortex interpolated directly from ECMWF 2.5 degree data set shows that the vortex was just too weak before the landfall. The maximum winds near the surface from numerical simulations (the lower panel of Figure 7) are both weaker than the instantaneous maximum wind estimated from observation (the dots), but they are much closer to the averaged maximum wind also estimated from observation.

4. Summary and discussion

In this initial attempt to compute surface wind fields for storm surge and ocean wave models, the conclusions that are based on the results of the above-described experiments are summarized below.

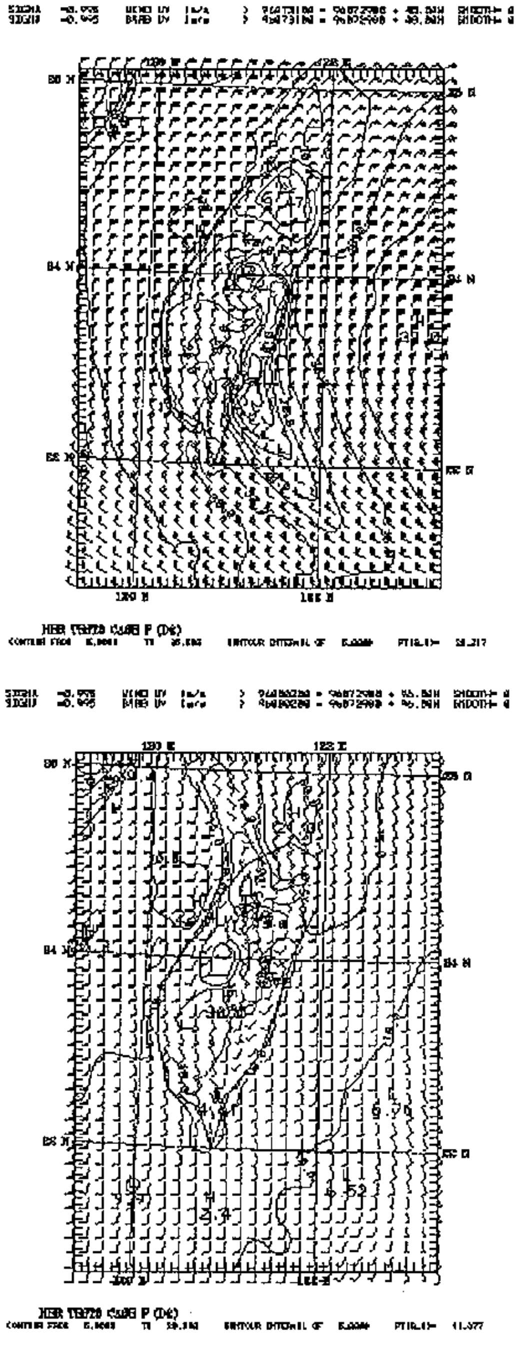

Figure 3. The near-surface wind patterns over Taiwan and its immediate vicinity during the southeastern wake stage (upper) and the northwestern wake stage (lower).

- The Central Mountain Range on the Island of Taiwan exerted a significant role in modifying the path and structure of Typhoon Herb as suggested by numerical experiments.

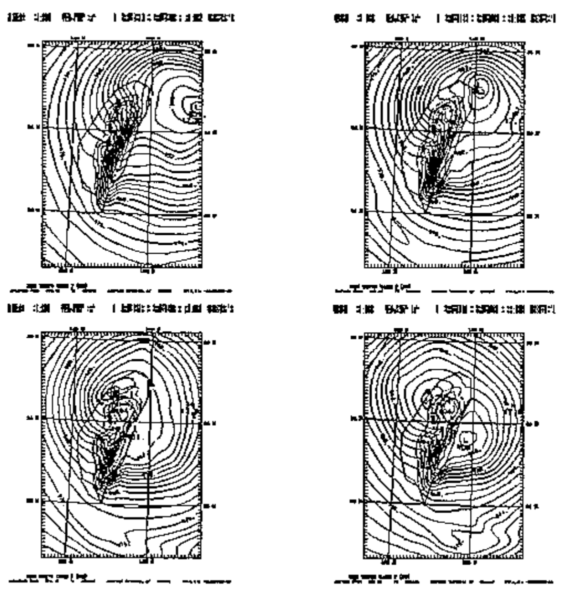

Figure 4. The surface pressure patterns during the transit of Typhoon Herb at 12Z (upper left), 14Z (upper right), 16Z (lower left), and 18z (lower right) 31/7/1996 over Taiwan and its immediate vicinity.

- Before Herb reached the island, it gyrated over the western Pacific as it moved in a northwestern direction.
- Because of its gyration and the influence of the mountainous island on it, the circulation of typhoon were not consistently circular and cannot be easily provided by other means than a numerical model with sufficient resolution.
- For operational forecasts of storm surges and ocean waves, an accurate surface wind field is crucial, and such fields have high spacial and temporal variability as shown in this case. Thus, surface wind fields should be obtained from predictions of numerical models with particular care in the lower atmosphere.

REFERENCES

Betts, A. K., and M. J. Miller, 1993: The Betts-Miller scheme. *The Representation of Cumulus Convection in Numerical Models, Meteor. Monogr.*, No. 46, Amer. Meteor. Soc., 107-121.

Dudhia, J., 1989: Numerical study of convection observed during the winter monsoon experiment using a mesoscale two-dimensional model. *J. Atmos. Sci.*, **46**, 3077-3107.

Hong, S.-Y. and H.-L. Pan, 1996: Nonlocal boundary layer vertical diffusion in a medium-range forecast model. *Mon. Wea. Rev.*, **124**, 2322-2339.

Smith, R.B., and D.F. Smith, 1995: Pseudo inviscid wake formation by mountain in shallow-water flow with a drifting vortex. *J. Atmos. Sci.*, **52**, 436-454.

Troen, I., and L. Mahrt, 1986: A simple model of the atmospheric boundary layer: Sensitivity to surface evaporation. *Boundary Layer Meteo.*, **37**, 129-148.

Shieh, S.-L., Wang, S.-T., M.-D. Cheng, and T.-C. Yeh, 1997: *User's Guide (2) for Typhoon Forecasting in the Taiwan Area* (in Chinese), Res. Rep. CWB85-1M-01, 381 pp.

Wang, S.-T., 1980: *Prediction of the Behavior and Strength of Typhoons in Taiwan and its Vicinity* (in Chinese), Res. Rep. 108, National Research Council, Taipei, Taiwan, ROC.

Authors:

Hsiao-ming Hsu
National Center for Atmospheric Research
P.O. Box 3000
Boulder, Colorado, USA
303-497-8455
Hsu@ucar.edu

Yueh-jiuan G. Hsu
Central Weather Bureau
64 Kung Yuan Rd.,
Taipei, Taiwan, ROC
2-2349-1190
Beng@cwb.gov.tw

Beng-chun Lee
Central Weather Bureau
64 Kung Yuan Rd.,
Taipei, Taiwan, ROC
2-2349-1191
Glory@gwya.cwb.gov.tw

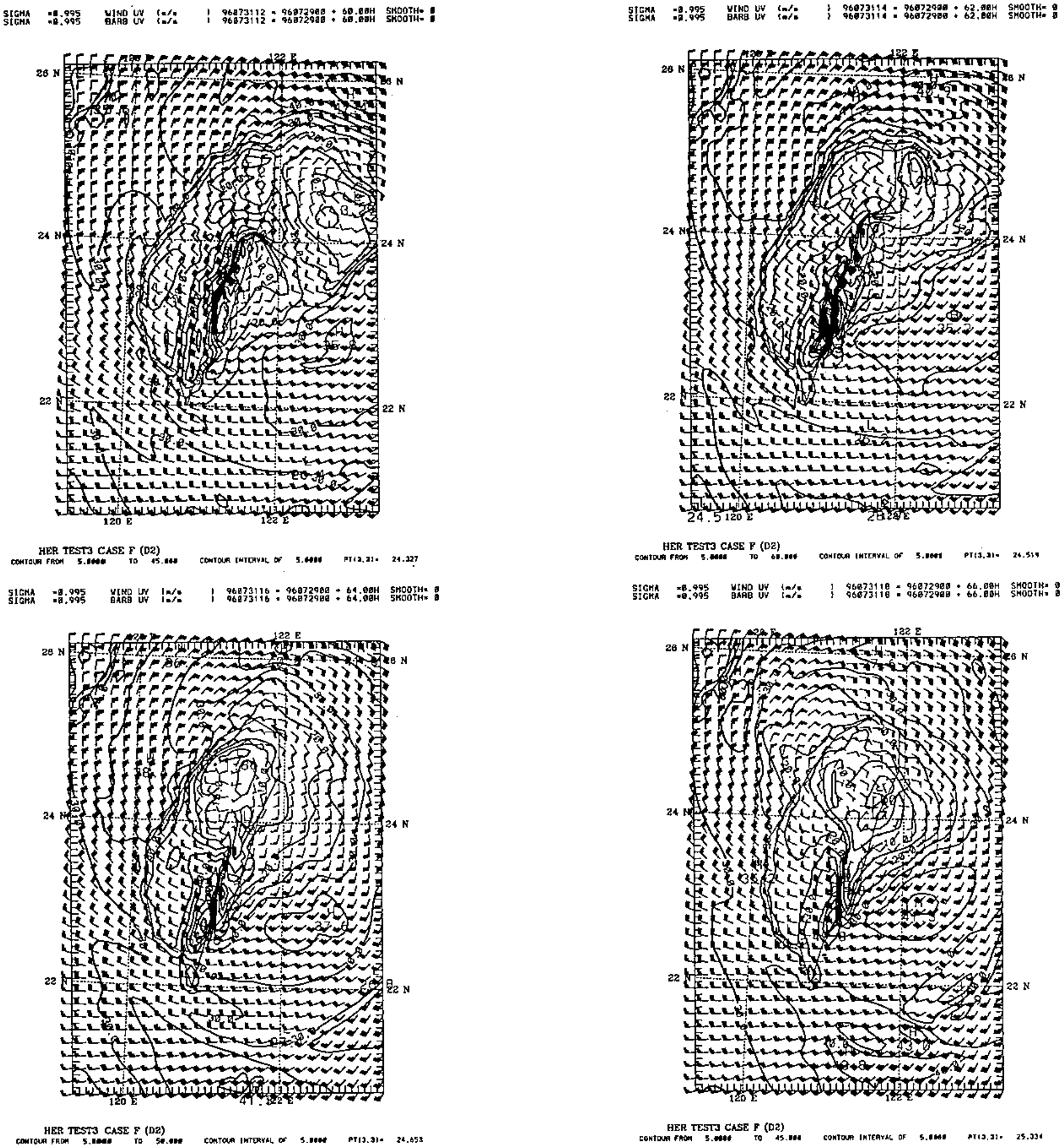

Figure 5. The near-surface wind patterns during the transit of Typhoon Herb at 12Z (upper left), 14Z (upper right), 16Z (lower left), and 18Z (lower right) 31/7/1996 over Taiwan and its immediate vicinity.

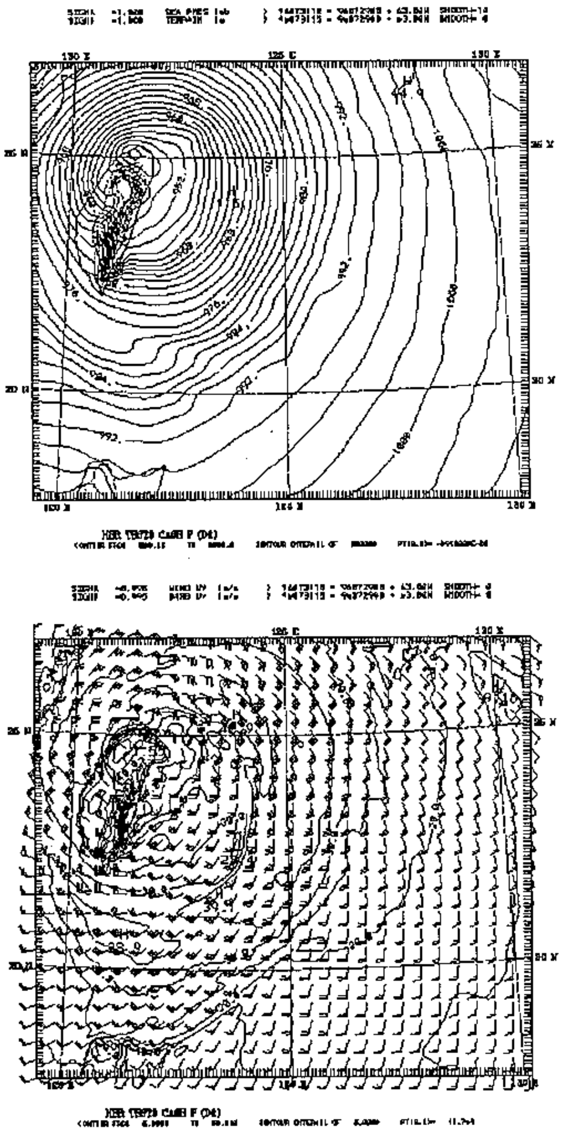

Figure 6. The surface pressure (upper) and near-surface wind (lower) patterns in the middle of the transit of Herb at 15Z 31/7/1996.

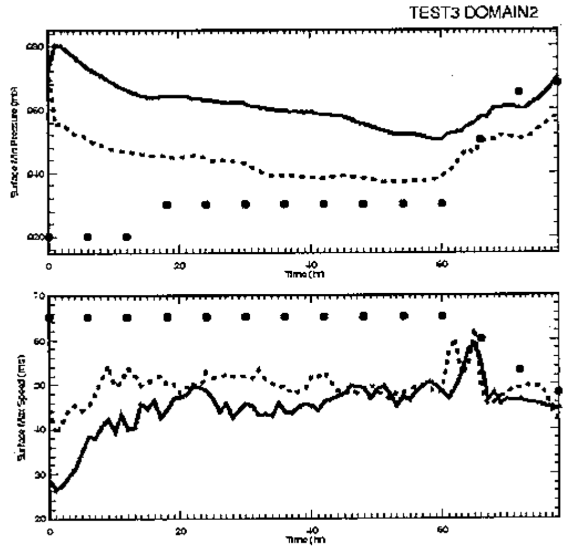

Figure 7. The time series of the minimum surface pressure (upper) and the maximum near-surface wind speed (lower) between 00Z 29/7/1996 and 06Z 1/8/1996. The solid and dashed lines are for the experiments ORIV and MODV, respectively. The dots are observations.